ELSEVIER

Journal of Photochemistry and Photobiology A: Chemistry 145 (2001) 215–222

Journal of Photochemistry and Photobiology A:Chemistry

www.elsevier.com/locate/jphotochem

Laser-induced decomposition and ablation dynamics studied by nanosecond interferometry 3. A polyurethane film

Tomokazu Masubuchi [a], Hiroshi Fukumura [a,1], Hiroshi Masuhara [a,*], Kenkichi Suzuki [b], Nobuaki Hayashi [b]

[a] *Department of Applied Physics, Osaka University, Suita, Osaka 565-0871, Japan*
[b] *Displays, Hitachi Ltd., Kokubunji, Tokyo 185-8601, Japan*

Abstract

A polyurethane sample film was prepared by adding phenol resin as a structural stabilizer and its laser ablation dynamics was studied upon excimer laser irradiation. The ablation threshold by 248 nm excitation was determined to be 40 mJ/cm^2 and no appreciable debris was left. The etch depth increases with the fluence and reaches 0.5 μm at the fluence of 1 J/cm^2. Time-resolved interferometric images were measured in the nanosecond to microsecond time region under surface and internal optical alignments. The film was decomposed efficiently into debris, fragments, aggregates, and so on which are smaller than the wavelength, as observed images were not disturbed by the decomposed products. At the fluence of 310 mJ/cm^2, etching proceeds fast during the initial half of the excitation laser pulse, but stopped at the late stage of the pulse. The direct measurement of transient absorbance change at 248 nm explains that ejected products still absorb the excitation photons and interrupt a further etching. Laser-induced expansion was not observed above the ablation threshold, while below the value an expansion forms a bump and followed by rapid contraction. The morphological behavior is quite different from that of usual photothermal expansion and contraction dynamics observed for poly(methyl methacrylate) and polystyrene, hence it is considered that laser ablation is induced photochemically.

Keywords: Laser ablation; Polyurethane film; Laser-induced expansion; Nanosecond interferometry; Photochemical decomposition

1. Introduction

Laser photochemistry of organic materials by highly intense excitation has received much attention, as very unique photophysical and photochemical processes are induced and coupled with each other, constituting interesting and important research topics [1–3]. One of examples are studies on laser ablation where depletion of the ground state, cyclic multiphoton absorption, excited state annihilation, and so on are involved [4–13]. As a result, temperature elevation, thermochemical decomposition, vaporization, fragmentation, ejection, and subsequent generation of shock wave are observed. It is indeed important and interesting as laser photochemistry to understand how electronic excitation of molecules in materials evolves to morphological changes [14]. Since the processes are induced in short time ranges, time-resolved measurements are very useful to interrogate the transient processes in laser ablation. Actually, a lot of time-resolved methods have been applied; picosecond anti-Stokes coherent Raman scattering spectroscopy [15,16], time-resolved absorption [13,17–20] and emission spectroscopy [17,18], transient absorbance measurement at the excitation wavelength [21,22], and time-resolved optical thermometry [23]. On the basis of systematic studies using these methods, some transient species and their dynamic processes in laser ablation phenomena have been clarified and considered.

Now it is strongly desired that the microscopic dynamic processes are connected to each other and integrated to etch depth data for understanding morphological dynamics leading to etched surface profile. Time-resolved photography [24–26] and time-resolved surface light scattering imaging [14] have been developed in order to bridge the gap between photoprimary processes and ablation behavior. The other techniques we have developed is a nanosecond time-resolved interferometry [27]. This can interrogate rapid and small expansion and contraction behavior

* Corresponding author.
E-mail address: masuhara@ap.eng.osaka-u.ac.jp (H. Masuhara).
[1] Present address: Department of Chemistry, Tohoku University, Sendai, Miyagi 980-8578, Japan.

1010-6030/01/$ – see front matter
PII: S1010-6030(01)00585-8

occurring during or just after laser excitation with high sensitivity (∼10 nm) and high temporal resolution (∼10 ns). The principle is simple; a Michelson interferometer has been developed to a pump-probe measurement. It is now possible to follow the dynamics from electronic excitation relaxation to volume expansion and contraction of sample films.

By using the nanosecond interferometry, we have succeeded in demonstrating nanosecond temporal evolution of nanometer morphological changes of several different polymer and dye films. In the case of poly(methyl methacrylate) (PMMA) films with [28] and without dopants [29], expansion of the films prior to the explosive ejection of ablated fragments was observed during the excimer laser pulse. Even below the ablation threshold, transient expansion takes place which is followed by slow contraction to a flat surface. Under a certain condition, glass–rubber transition of PMMA film was observed during laser-induced expansion. Surface displacement dynamics due to laser-induced decomposition of triazenopolymer and nitrocellulose films were directly measured [30,31]. Quite recently, the relevant study is being extended to various polymer films to reveal how ablation and expansion/contraction dynamics depend on excitation wavelength and to elucidate photochemical and photothermal mechanisms.

In the present work, we examine polyurethane film which is practically important and widely used as industrial and commercial products. Some experiments have been recently conducted, where the film is used as electronic materials and laser microfabrication [32]. It was found that polyurethane film has a rather low ablation threshold and high etching rate, namely, etch depth attained by one-shot excitation is large. The results suggest that an interesting etching mechanism holds for polyurethane and unique decomposition processes are involved. Here, the nanosecond interferometry is applied for the first time to the polyurethane film, and the laser-induced morphological dynamics is revealed and discussed.

2. Experimental

2.1. Sample

Polyurethane (Isomelt 1500, Schenectady Chemicals, USA) was used without further purification. As it does not form a stable film, phenol resin (Alnovel PN430, Hoechst) was added as a binder polymer. A 15 wt.% chlorobenzene (Wako, 99.0% purity) solution of polyurethane and phenol resin where the weight ratio of the former to the latter is 4:1 was prepared and spin-coated onto two kinds of quartz plates under the rotation condition of 250 rpm for initial 10 s and 4500 rpm for succeeding 60 s. The film was heated at 100°C for 2 h in vacuum to remove residual chlorobenzene. The film thickness was usually 1 μm, absorption coefficient at the excitation wavelength is 12.2 μm^{-1}, and its absorbance at 248 nm = 5.3. Chemical structure and

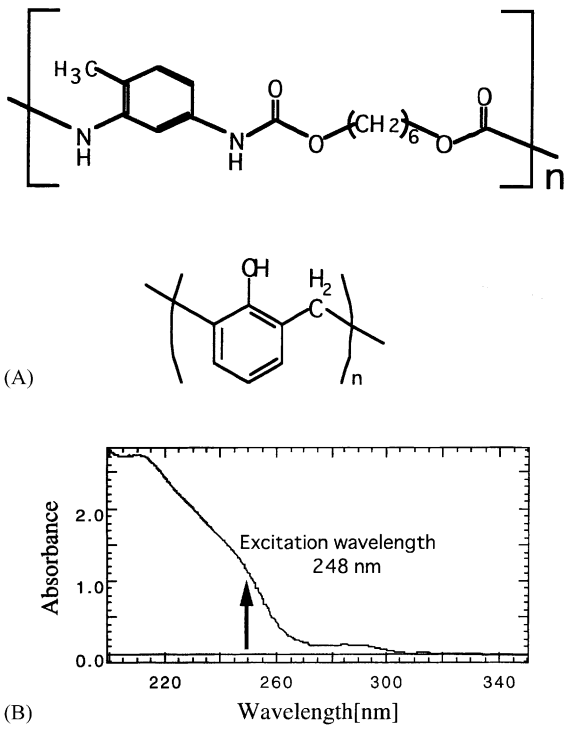

Fig. 1. (A) Chemical structures of polyurethane (upper) and phenol resin (lower). (B) UV absorption spectra of the polyurethane/phenol resin sample film.

absorption spectrum of the sample film with thickness of 230 nm are given in Fig. 1. The refractive index of the sample film was estimated to be 1.66 by elipsometry.

2.2. Ablation experiment

A KrF excimer laser (Lambda Physik Lextra 200, 248 nm, 30 ns FWHM) was used as an excitation pulse for inducing expansion/contraction, decomposition, and ablation. The fluence was adjusted with partially transmitting laser mirrors, and was monitored by a joulemeter (Gentec, ED-200) with an oscilloscope (Hewlett-Packard, HP54522A). A central area of the excimer laser pattern with a homogeneous intensity distribution was chosen with an appropriate aperture and then focused onto the sample surface by using a quartz lens ($f = 200$ mm). Fresh surface of the sample film was examined in every measurement. Etch depth was measured by a surface depth profiler (Sloan, Dektak 3). All experiments were done in air at room temperature.

2.3. Nanosecond time-resolved interferometry

The nanosecond time-resolved interferometry applied here is the same as reported before [27]. Briefly, the second harmonic pulse of a Q-switched Nd^{3+}:YAG laser (Continuum Surelite I, 532 nm, 10 ns FWHM) was used as a probe light for the Michelson-type interferometer to measure excimer laser-induced morphological changes of

the present film. Interference patterns were acquired by a CCD camera. Time-resolved measurement was carried out by controlling the delay time (Δt) between excitation and probe laser pulses with a digital delay/pulse generator (Stanford Research System, DG 535). The delay time was monitored shot-by-shot by a digital oscilloscope. Here, we define $\Delta t = 0$ when the peaks of both laser pulses coincide with each other. All data were obtained by one-shot measurement to avoid effects by exciting photoproducts formed by previous irradiation.

We adopted two kinds of quartz substrate: surface and internal configurations, as in the previous works [30]. In case of the surface configuration, fringe pattern results from an interference between the reference light from a standard reference mirror and the light reflected at the polymer surface. In order to avoid a disturbing interference due to a light reflected at the back surface of the quartz plate, a plate whose two surfaces are not parallel with each other was used. However, fragments or gaseous products are sometimes ejected from the sample film upon laser ablation and may vary the effective optical path length of the reflected light. The disturbance by the ejected products will lead to overestimation of the surface displacement of the irradiated polymer film. To overcome this problem, we use the internal configuration where the surface of the quartz substrate, facing to the polymer film, and the back surface of the quartz plate are almost in parallel. The reflected light from the latter surface interferes with the reflected one from the polymer surface, generating interference fringe patterns. Neither changes in thickness and/or refractive index of the polymer film nor refractive index change due to ejected fragments or gaseous products are included in the shift of the interference patterns, as optical path is common to reference and probe light beams.

In the experiment, a movement of the fringe to the left and right directions represent an expansion and etching of polymer film, respectively, which was confirmed by adjusting the optical condition. A shift of one fringe spacing corresponds to 266 nm, a half-wavelength of the probe laser, so that we can estimate the amplitude of surface displacement as a function of delay time.

2.4. Transient absorption measurement at 248 nm excitation wavelength

Transmittance change of sample film at 248 nm during the excimer laser irradiation was measured as reported before [21]. Excimer laser light was separated into two by a quartz plate: very weak one as a reference light and another for exciting the polymer film. The reference light and the transmitted light after excitation were measured by two photodiodes. Their signals were monitored shot-by-shot by a digital oscilloscope and compared with each other, and transient absorbance at 248 nm during the excitation was calculated.

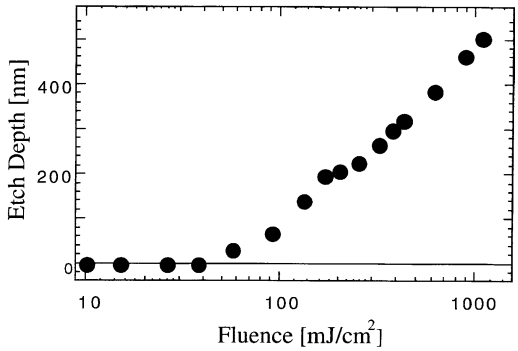

Fig. 2. Etch depth profile of polyurethane/phenol resin sample film obtained with 248 nm excimer laser one-shot irradiation.

3. Results and discussion

3.1. Etch depth

Fluence dependence of etch depth of the sample film is given in Fig. 2, where ablation threshold is determined to be 40 mJ/cm^2. The threshold is rather low compared to conventional polymers such as neat PMMA [29] and polystyrene (PS) [33]. It is worth noting that the etch depth increases monotonously with the laser fluence without saturation and it reaches 0.5 μm at the fluence of 1 J/cm^2. This suggests that laser-induced decomposition to small molecules and fragments proceeds efficiently and no appreciable amount of debris scattering the probe pulse is left. Application of nanosecond interferometry will reveal when ablation is started and what kinds of primary processes are involved. Below the threshold, it is generally considered that nothing takes place, but now this simple expectation can be confirmed.

3.2. Nanosecond interferometric images

As pointed out in Section 2, ejected gaseous molecules and small fragments change refractive index in the optical path and modify interferometric images. Here, we have applied both surface and internal configurations and estimate precisely etching dynamics. In Figs. 3 and 4, nanosecond interferometric images of the sample film at 310 mJ/cm^2 above the ablation threshold are shown as representative examples.

Firstly, we should point out that interferometric images are always observed clearly. This means that the decomposed debris, ejected fragments, and so on are all smaller than light wavelength and do not scatter the probe pulse substantially. Efficient decomposition is achieved by one-shot excitation. This is one of advantages of polyurethane ablation compared to PMMA and PS films, as in the latter case ejected materials are larger and shield the probe light, giving no meaningful image after ablation.

Secondly, even minus delay time, namely, at the initial half of the excitation pulse, the fringe shift to the right side is started, which was detected with both configurations. Around zero delay time, the shift was almost stopped and

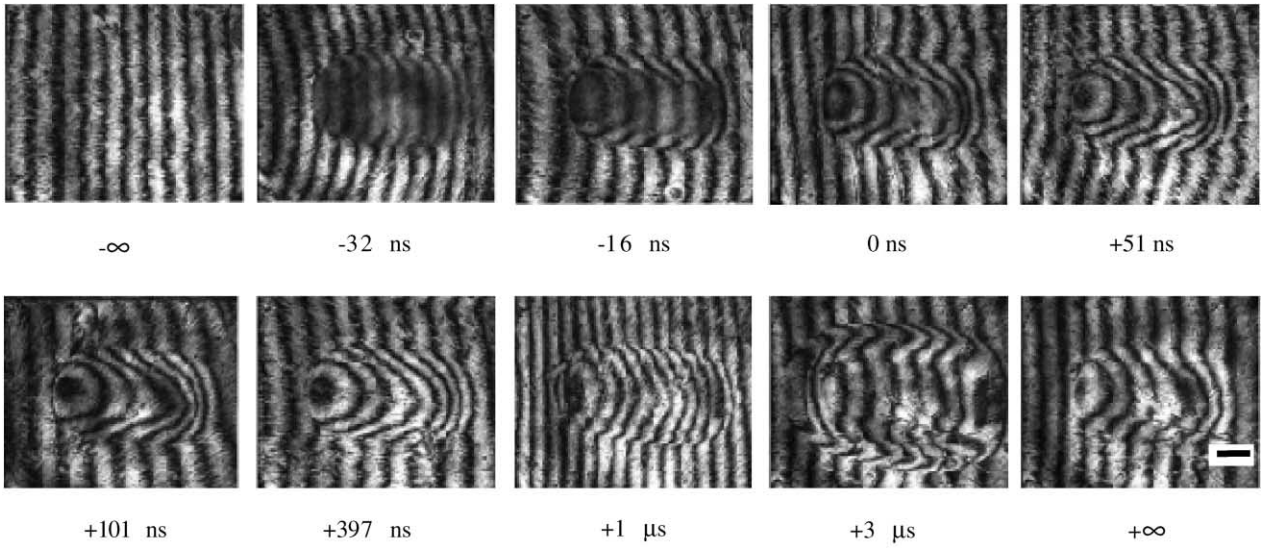

Fig. 3. Nanosecond time-resolved interferometric images of polyurethane/phenol resin sample film on a wedged quartz plate at the fluence of 310 mJ/cm^2 above the ablation threshold, which was obtained with the surface configuration (see text). These images are taken shot-by-shot at a fresh area of the same sample film. The fringe shift to the right represents etching. Delay times are given in the figure. The black bar in the last photograph indicates 1 mm in the image.

no appreciable shift was observed later. Interferometric pattern changes from delay time to delay time, since the interrogated area of the film is sequentially shifted and the optical alignment is delicately changed. Thus, fringe patterns are not always similar. It is worth noting that an interesting large difference in images between both configurations appeared at 3 μs after excitation. Although the periodic pattern in the central irradiated area shifts always to the right side compared to non-irradiated area and patterns in both areas are connected monotonously in the boarder domains, sharp curves on the peripheral areas were observed only in an image acquired with the surface configurations. This characteristic curves propagated outside later, which was also never detected with the internal configuration. This is because an increase in effective optical path length is not compensated in the surface configuration as mentioned above. Thus, it is concluded that characteristic modification of interferometric patterns at 3 μs in Fig. 3 is due to refractive index change due to ejected gaseous and small molecules propagating from the central to peripheral parts.

Thirdly, laser-induced shift with the surface configuration is always larger than that with the internal configuration. This

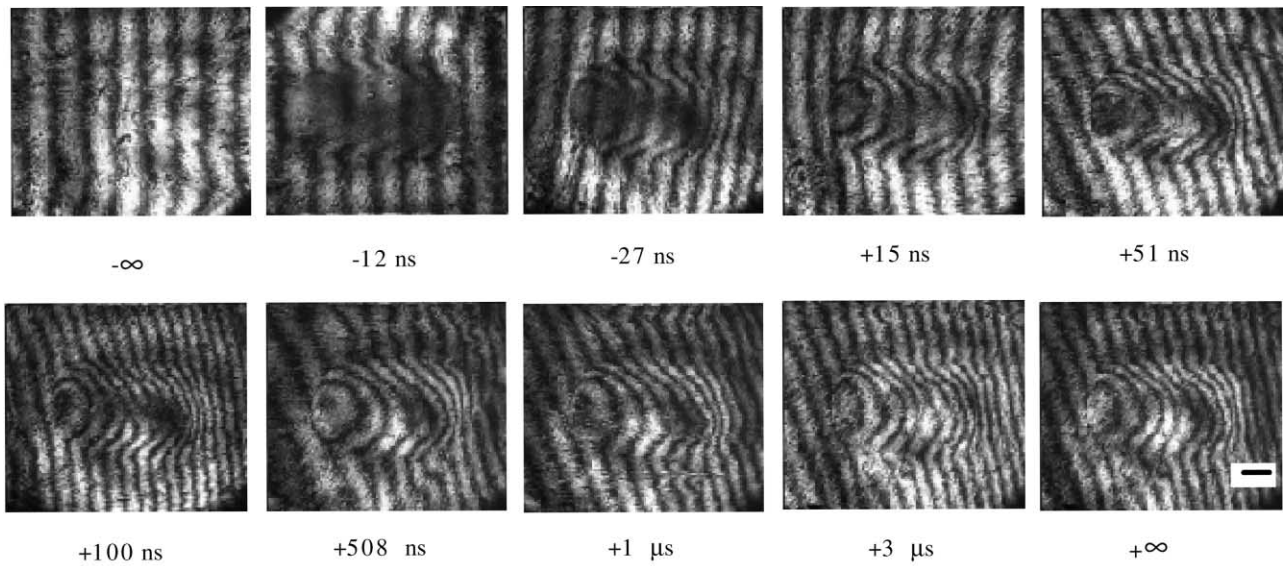

Fig. 4. Nanosecond time-resolved interferometric images of polyurethane/phenol resin sample film on a quartz plate with parallel surfaces at the fluence of 310 mJ/cm^2 above the ablation threshold, which was obtained with the internal configuration (see text). All other conditions are the same to those of Fig. 3.

is consistent with the above description about the image at 3 μs. The gaseous molecules and small fragments are ejected also at the top direction, so that effective refractive index along the monitoring path becomes large compared to air. This effect can be cancelled with the internal configuration, while not with the surface configuration [30]. Thus, apparent shift is larger with the surface configuration compared to the internal one.

Etching dynamics obtained by analyzing the images in Figs. 3 and 4 is summarized in Fig. 5, where the results at lower fluence are also included. The difference between etch depth estimated with both configurations is clearly shown for all the results. The depth with the surface configuration is always larger than that with internal one, and the difference is larger with increasing the fluence. At a few minutes after excitation the depth values obtained with both configurations are similar to each other, which means that gaseous molecules and small fragments diffuse out in this time range. The permanent etch depth was obtained to be 240, 90 and 70 nm for 310, 100 and 70 mJ/cm^2 excitation, respectively, and all those values are identical to those measured by a depth profiler. Thus, the results are quite reasonable and we can say that the present data are precise and reliable.

3.3. Etching dynamics above the ablation threshold

Now, we consider etching dynamics on the basis of the results with the internal configuration. Ablation is started at the initial stage of the excimer laser pulse, continued during excitation, almost saturated around 0 ns, and stopped completely when the excitation is finished. Furthermore, no appreciable expansion process was detected. It is noticeable that permanent etch is already attained at the end of the excitation pulse and no contraction is involved. This means the film is not heated appreciably suggesting negligible photothermal effect. In the case of photothermal ablation like in neat and doped films of PMMA and PS, expansion succeeds ablation, fragmented debris scatter the probe pulse giving

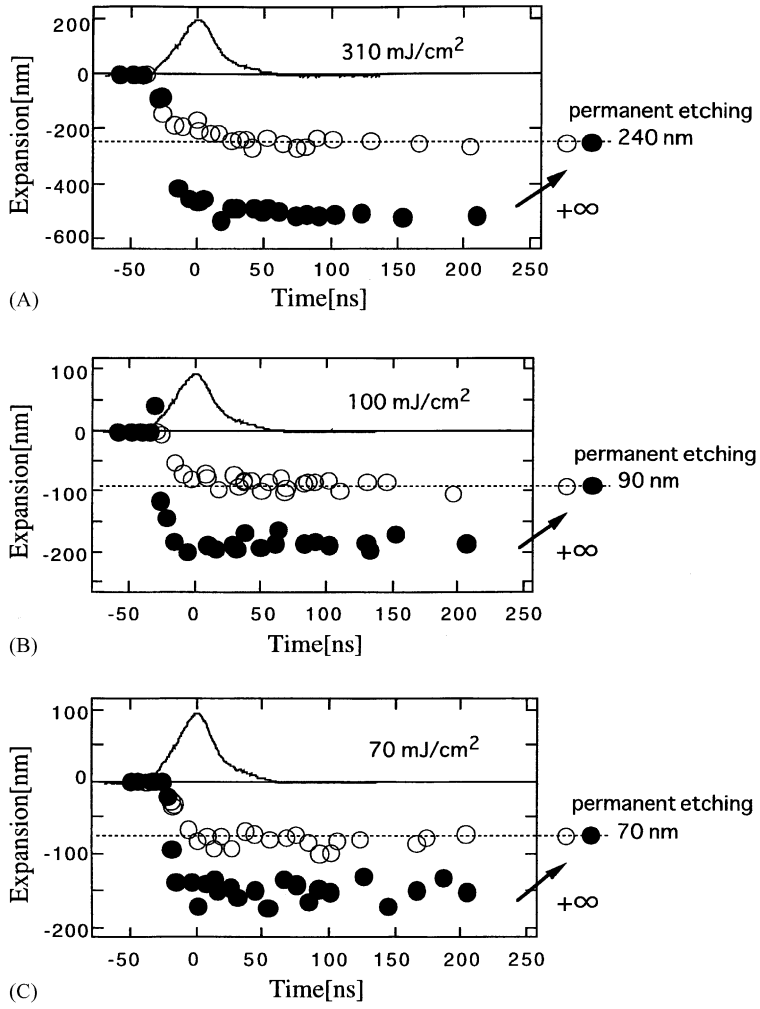

Fig. 5. Etching dynamics of polyurethane/phenol resin sample film above the ablation threshold with the surface (●) and internal (○) configurations. The dashed lines mean the permanent etch depth measured by depth profiler, while the solid curves represent the excimer laser pulse profiles. Laser fluence is: (A) 310 mJ/cm^2; (B) 100 mJ/cm^2; (C) 70 mJ/cm^2.

no image after ejection, and slow contraction is observed [25,28]. These results can be interpreted with photochemical decomposition mechanism. The average etching speed of the sample film is about a few nanometers/nanoseconds, and close to that of triazenopolymer film (∼10 nm/ns). Indeed, the latter polymer was decomposed directly from solid to gaseous products, and the etching process was finished during the excitation laser pulse [30]. The decomposition dynamics was dependent on the applied fluence, on which we concluded that the decomposition is induced dominantly via a photochemical pathway. On the other hand, doped nitrocellulose film underwent expansion and then exothermic self-sustaining decomposition, which was well explained in terms of photothermal ablation mechanism [31].

While ablation characteristics of the polyurethane sample film are clear, its etch rate, namely, etch depth per pulse, is not enough large. Even at the fluence of 1 J/cm^2 at 248 nm, the etch depth is around half-micrometer, which is smaller than conventional materials. One of the reasons will be that the etching is almost finished at about 0 ns and does not proceed at the late stages of the excitation pulse. In order to elucidate this problem, we have measured transient absorbance at the excitation wavelength itself. A thin film with thickness of 230 nm whose steady-state absorbance 1.23 was examined, as the absorbance at 248 nm is extremely large and no transmitted light was detected for the film with 1 μm thickness which is used for all the experiments here.

Transient absorbance change during excitation is shown as a function of the laser fluence in Fig. 6. Below and just above the ablation threshold, the absorbance does not change appreciably, which means the Lambert–Beer rule holds and non-linear absorption processes are not involved. At the fluence of 100 and 200 mJ/cm^2, the absorbance reduced with time, while sudden decrease in the absorbance was observed for the fluence of 250 and 310 mJ/cm^2. According to the results of Fig. 2, etch depth at 310 mJ/cm^2 is about 240 nm, and actually the present film with thickness of 230 nm was completely removed. The above interferometric study tells us this etch is almost finished around 0 ns. However, still appreciable absorbance was observed even at the latter half of the excitation pulse. This means that ejected small fragments and vaporized small molecules just above the quartz plate are responsible to the absorbance observed in the time range 0–40 ns. Its value is about two-thirds of the original absorbance and about 1.0, which is large enough to absorb most of the photons incident at the latter half of the 248 nm pulse. The sample film used here has a thickness of 1 μm and is thick enough to be ablated deeply, but the excitation pulse may be stopped at the surface layer. To achieve more efficient etch rate, photodecomposition to smaller molecules which do not give absorption at 248 nm is requested. Chemical design of polyurethane derivatives and/or new ablation condition such femtoseconds or short wavelength excitation will be useful.

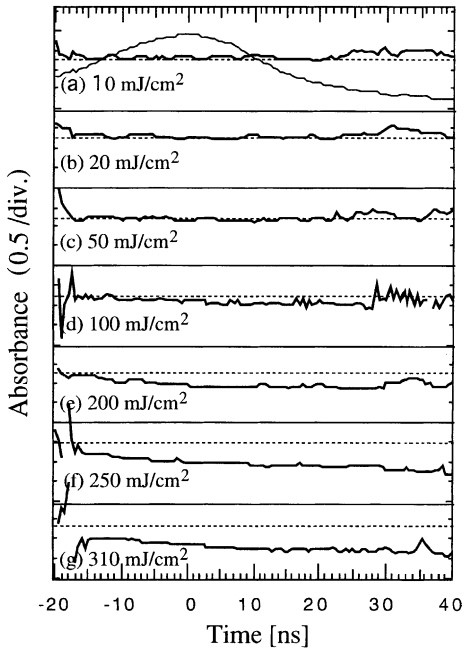

Fig. 6. Transient absorption change of polyurethane/phenol resin sample film at the excitation wavelength during the 248 nm excimer laser irradiation. The thin solid curve represents the excimer laser profile, while the dashed lines are steady-state absorbance measured by a conventional spectrophotometer.

3.4. Unusual expansion and contraction dynamics below the ablation threshold

When the film is excited at the fluence of 20 mJ/cm^2, the fringe shift to the left side was obtained at early delay times, while the original pattern was completely recovered at a few minutes after excitation. A series of images representing this dynamics are summarized in Fig. 7. The results show that the film underwent expansion and then contracted, recovering the original position. Their dynamics obtained by analyzing the data of Fig. 7 is presented in Fig. 8. The expansion amplitude is larger for 20 mJ/cm^2 than for 12 mJ/cm^2, but temporal behavior is similar to each other. The expansion starts at the initial half of the excimer laser peak and reaches maximum value around 50 ns, showing a bump, and then contraction is started and finished at about 1 μs.

This expansion behavior is easily accepted, since various polymer films we have studied by the present nanosecond interferometry show such fast expansion. Expansion rate is estimated to be 1 nm/ns. On the other hand, contraction behavior after 100 ns is quite different from that of neat PMMA and PS films where photothermal mechanism is most probable [29,33]. Contraction process should be controlled by cooling process, namely, thermal dissipation determines the time scale of contraction and usually takes place in the microsecond order. Actually, PMMA and PS films do not show any detectable contraction in the present time range. Consequently, the present result showing recovery of the original surface place in 1 μs cannot be explained

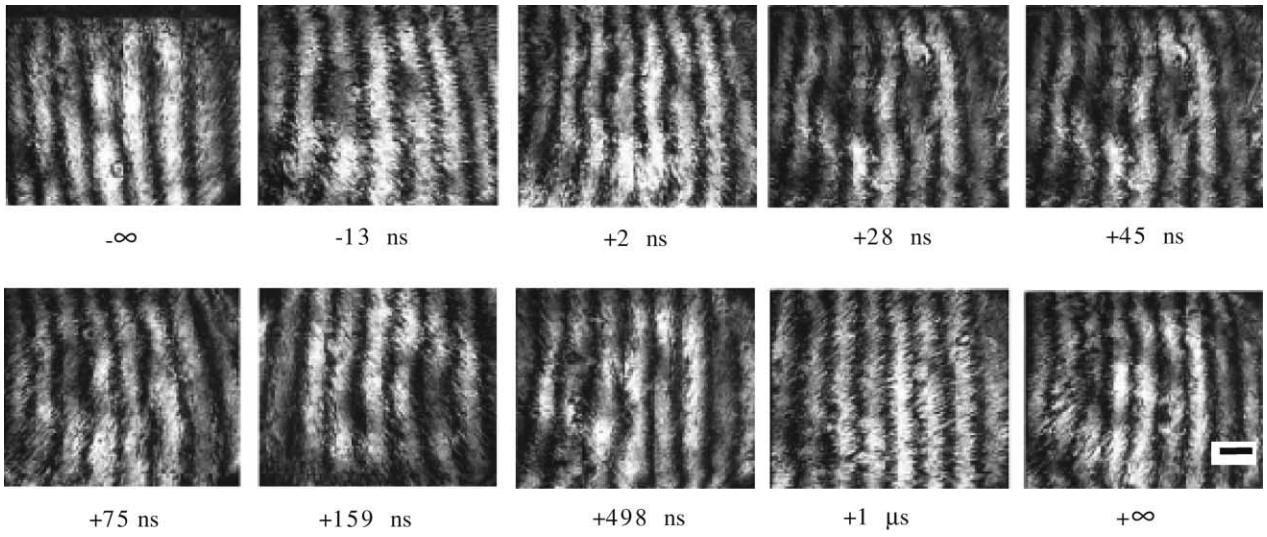

Fig. 7. Nanosecond time-resolved interferometric images of polyurethane/phenol resin sample film on a wedged quartz plate at the fluence of 20 mJ/cm^2 below the ablation threshold, which was obtained with the surface configuration (see text). The fringe shift to the left represents expansion. All other conditions are the same to those of Fig. 3.

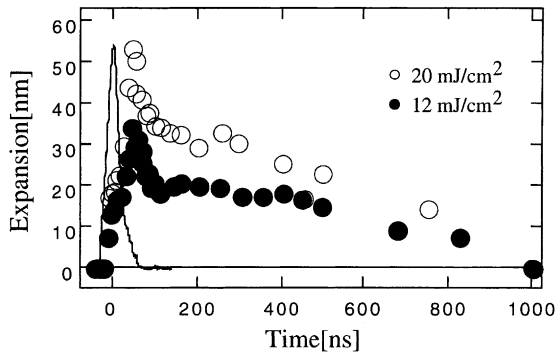

Fig. 8. Expansion and contraction dynamics of polyurethane/phenol resin sample film below the ablation threshold. Laser fluence is given in the figure. The solid curve represents the excimer laser profile.

by the thermal dissipation model. We have simulated numerically contraction dynamics using thermochemical parameters such as heat capacity, heat conductance, density, and thermal expansion coefficient, but could not reproduce the rapid decay in sub-microsecond time domains as observed here. Thus, photochemical mechanism we proposed above is not inconsistent with the contraction dynamics.

At the present stage of investigation, we interpret the contraction in terms of mechanical and polymer structural viewpoints. Fast expansion may result in overshooting, but does not undergo oscillation, which is quite different from mechanical response of metals and crystals. Structural relaxation of interpenetrating polymer chains is induced, associated free volume is re-distributed, and photochemical degradation proceeds. All these dynamic behaviors will be microscopic mechanism of a bump followed by fast contraction.

Acknowledgements

The present work is partly supported by the Grand-in-Aid for Scientific Research on Priority Area (B) on “Laser Chemistry of Single Nanometer Organic Particles” from the Ministry of Education, Science, Sports, and Culture of Japan (10207204).

References

[1] T. Asahi, H. Masuhara, Chem. Lett. (1997) 1165.
[2] Y. Tsuboi, H. Akita, K. Yamada, A. Itaya, Jpn. J. Appl. Phys. 36 (1997) L1048.
[3] G. Gery, H. Fukumura, H. Masuhara, J. Phys. Chem. B 101 (1997) 3698.
[4] H. Fukumura, H. Masuhara, Chem. Phys. Lett. 221 (1994) 373.
[5] H. Fukumura, N. Mibuka, S. Eura, H. Masuhara, N. Nishi, J. Phys. Chem. 97 (1993) 13761.
[6] Y. Kawamura, K. Toyoda, S. Namba, Appl. Phys. Lett. 40 (1982) 374.
[7] R. Srinivasan, V. Mayne-Banton, Appl. Phys. Lett. 41 (1982) 576.
[8] R. Srinivasan, W.J. Leigh, J. Am. Chem. Soc. 104 (1982) 6784.
[9] R. Srinivasan, B. Baren, Chem. Rev. 89 (1989) 1303.
[10] J.C. Miller, Laser Ablation — Principles and Applications, Springer, Berlin, 1994.
[11] Y. Tsuboi, H. Fukumura, H. Masuhara, J. Phys. Chem. 99 (1995) 10305.
[12] Y. Tsuboi, K. Hatanaka, H. Fukumura, H. Masuhara, J. Phys. Chem. 98 (1994) 11237.
[13] Y. Tsuboi, K. Hatanaka, H. Fukumura, H. Masuhara, J. Phys. Chem. A 102 (1998) 1661.
[14] Y. Hosokawa, M. Yashiro, T. Asahi, H. Fukumura, H. Masuhara, Appl. Surf. Sci. 154–155 (2000) 192.
[15] D.E. Hare, J. Franken, D.D. Dlott, J. Appl. Phys. 77 (1995) 5950.
[16] S.A. Hambir, J. Franken, D.E. Hare, E.L. Chronister, B.J. Baer, D.D. Dlott, J. Appl. Phys. 81 (1997) 2157.
[17] H. Fukumura, E. Takahashi, H. Masuhara, J. Phys. Chem. 99 (1995) 750.

[18] H. Fujiwara, Y. Nakajima, H. Fukumura, H. Masuhara, J. Phys. Chem. 99 (1995) 11481.
[19] K. Hatanaka, M. Kawao, Y. Tsuboi, H. Fukumura, H. Masuhara, J. Appl. Phys. 82 (1997) 5799.
[20] H. Fukumura, K. Hamano, H. Masuhara, J. Phys. Chem. 97 (1993) 12110.
[21] H. Fujiwara, T. Hayashi, H. Fukumura, H. Masuhara, Appl. Phys. Lett. 64 (1994) 2451.
[22] H. Fujiwara, H. Fukumoto, H. Fukumura, H. Masuhara, Res. Chem. Intermed. 24 (1998) 879.
[23] I.-Y.S. Lee, X. Wen, W.A. Tolbert, D.D. Dlott, M.D. Doxtader, R.J. Arnold, Appl. Phys. 72 (1992) 2440.
[24] R. Srinivasan, B. Braren, K.G. Cassey, M. Yeh, Appl. Phys. 55 (1989) 2790.
[25] L.S. Bennett, T. Lippert, H. Furutani, H. Fukumura, H. Masuhara, Appl. Phys. A 63 (1996) 327.
[26] Y. Tsuboi, K. Hatanaka, H. Masuhara, Appl. Phys. Lett. 64 (1994) 2745.
[27] H. Furutani, H. Fukumura, H. Masuhara, Appl. Phys. Lett. 65 (1994) 3413.
[28] H. Furutani, H. Fukumura, H. Masuhara, J. Phys. Chem. 100 (1996) 6871.
[29] T. Masubuchi, H. Furutani, H. Fukumura, H. Masuhara, Chem. Phys. Chem. 1 (2000) 137.
[30] H. Furutani, H. Fukumura, H. Masuhara, T. Lippert, A. Yabe, J. Phys. Chem. A 101 (1997) 5742.
[31] H. Furutani, H. Fukumura, H. Masuhara, S. Kambara, T. Kitaguchi, H. Tsukada, T. Ozawa, J. Phys. Chem. B 102 (1998) 3395.
[32] K. Suzuki, M. Matsuda, T. Ogino, N. Hayashi, T. Terabayashi, K. Amemiya, SPIE Proc. 16 (1997) 2992.
[33] T. Mito, T. Masubuchi, T. Tada, H. Fukumura, H. Masuhara, J. Photosci. 6 (1999) 109.